Construction of G^1 planar Hermite interpolants with prescribed arc lengths

Rida T. Farouki
Department of Mechanical and Aerospace Engineering,
University of California, Davis, CA 95616, USA.

Abstract

The problem of constructing a plane polynomial curve with given end points and end tangents, and a specified arc length, is addressed. The solution employs planar quintic Pythagorean–hodograph (PH) curves with equal–magnitude end derivatives. By reduction to canonical form it is shown that, in this context, the problem can be expressed in terms of finding the real solutions to a system of three quadratic equations in three variables. This system admits further reduction to just a single univariate biquadratic equation, which always has positive roots. It is found that this construction of G^1 Hermite interpolants of specified arc length admits two formal solutions — of which one has attractive shape properties, and the other must be discarded due to undesired looping behavior. The algorithm developed herein offers a simple and efficient closed–form solution to a fundamental constructive geometry problem that avoids the need for iterative numerical methods.

Keywords: Geometric Hermite interpolation; prescribed arc length; Pythagorean–hodograph curves; complex representation; polynomial roots.

e–mail: farouki@ucdavis.edu

1 Introduction

It is, in general, impossible to exactly specify or compute the arc length of a free–form curve segment. Whereas most curve construction methods rely on the interpolation of discrete data — points, tangents, curvatures, etc. — the imposition of a desired total arc length is an integral or "global" constraint, that generally necessitates the use of iterative approximate methods.

The *Pythagorean–hodograph* (PH) *curves* are unique, among polynomial curves, in having arc lengths that are exactly determined by simple algebraic expressions in their coefficients [8]. Although this property has been exploited in real–time motion control applications [11, 12, 15] for PH curve paths, there has been little investigation thus far of the *construction* of smooth paths with specified arc lengths. One application arises [20] in the shape reconstruction of smooth surfaces using the *Morphosense*, a ribbon–like device incorporating orientation sensors at known distances along its length. Iterative numerical methods were employed, in this context, to construct a spatial C^2 PH quintic spline with prescribed arc lengths between nodal points. Other contexts in which precise control over path arc lengths may be desired include the layout of carbon fiber in composite materials manufacturing, and in the deposition, curing, or sintering of materials in layered manufacturing processes.

The aim of this paper is to formulate a comprehensive solution procedure for the problem of interpolating G^1 data (end points and tangents) by planar PH quintics of a prescribed arc length. It is known [13] that, in general, the C^1 planar PH quintic interpolation problem admits four distinct solutions. Relaxing from C^1 to G^1 end conditions yields two free scalar parameters, of which one is used to achieve the desired arc length, and the other is fixed by imposing end derivatives of equal magnitude (with the desirable consequence that symmetric G^1 data yield symmetric interpolants). It is shown below that this problem admits an attractively simple and efficient closed–form solution, requiring little more than the solution of a quadratic equation.

The counterpart problem of interpolating spatial G^1 data by PH curves of prescribed arc length is deferred to a future study. It is known that spatial PH quintic interpolants to C^1 data incorporate two free parameters, of which one can be used to fix the arc length within a certain range [9, 10]. Relaxing to G^1 data will yield a total of four free parameters (or three if the end derivatives are again assumed to be of equal magnitude), and careful consideration must be made of their use in optimizing the interpolant shape.

Although geometric Hermite interpolation has been investigated by many

authors — e.g., [4, 6, 16, 17, 18, 19, 21, 26, 28, 29, 30, 31] — the problems considered typically address only discrete local data. Satisfaction of global (integral) geometrical constraints poses a much more challenging task, if only because of the lack of simple closed–form expressions for the curve integral properties under consideration. For example [32] addresses the construction of planar cubic G^1 interpolants that minimize the elastic strain energy (i.e., the integral of the squared curvature with respect to arc length) by varying the end derivative magnitudes. To make the problem tractable, however, the energy integral is replaced by an approximation that is only valid in the weak curvature limit. Similarly [23] presents a method to construct planar quintic interpolants to G^2 Hermite data that minimize the energy integral, but this integral is again approximated, and an iterative numerical method is required to determine the solutions. The problem considered herein is distinguished by the fact that the integral constraint admits an exact closed–form expression, and the solutions are obtained by a simple closed–form algorithm.

The plan for the remainder of this paper is as follows. Section 2 reviews basic properties of planar PH curves, and the complex representation used in their construction. The interpolation of G^1 data, subject to the constraint of a specified interpolant arc length, is then thoroughly analyzed in Section 3. An algorithm that summarizes the solution procedure is outlined in Section 4, and several computed examples are presented to illustrate its performance. Finally, Section 5 briefly summarizes the contributions of the present study, and identifies possible directions for further investigation.

2 Planar Pythagorean-hodograph curves

A planar polynomial Pythagorean–hodograph (PH) curve $\mathbf{r}(\xi) = (x(\xi), y(\xi))$, $\xi \in [\,0, 1\,]$ has derivative components $x'(\xi), y'(\xi)$ satisfying [14] the condition

$$x'^2(\xi) + y'^2(\xi) \;=\; \sigma^2(\xi) \tag{1}$$

for some polynomial $\sigma(\xi)$, which specifies the *parametric speed* of $\mathbf{r}(\xi)$, i.e., the derivative of the arc length s with respect to the curve parameter ξ. This feature endows PH curves with many attractive computational properties — they have rational unit tangents and normals, curvatures, and offset curves; their arc lengths are exactly computable; and they are ideally suited to real–time precision motion control applications [8].

For a primitive curve, with $\gcd(x'(\xi), y'(\xi)) = \text{constant}$, a sufficient and necessary condition for the satisfaction of (1) is that $x'(\xi)$, $y'(\xi)$ should be expressible in terms of polynomials $u(\xi)$, $v(\xi)$ in the form

$$x'(\xi) \;=\; u^2(\xi) - v^2(\xi)\,, \quad y'(\xi) \;=\; 2\,u(\xi)v(\xi)\,.$$

This structure is embodied in the complex representation [7], in which a PH curve of degree $n = 2m+1$ is generated from a degree–m complex polynomial

$$\mathbf{w}(\xi) \;=\; u(\xi) + \mathrm{i}\,v(\xi) \;=\; \sum_{k=0}^{m} \mathbf{w}_k \binom{m}{k} (1-\xi)^{m-k}\xi^k$$

with Bernstein coefficients $\mathbf{w}_k = u_k + \mathrm{i}\,v_k$ by integration of the expression

$$\mathbf{r}'(\xi) \;=\; \mathbf{w}^2(\xi)\,. \tag{2}$$

The parametric speed, unit tangent, and curvature of $\mathbf{r}(\xi)$ may be formulated [7] in terms of $\mathbf{w}(\xi)$ as

$$\sigma(\xi) \;=\; |\mathbf{w}(\xi)|^2\,, \quad \mathbf{t}(\xi) \;=\; \frac{\mathbf{w}^2(\xi)}{\sigma(\xi)}\,, \quad \kappa(\xi) \;=\; 2\,\frac{\mathrm{Im}(\overline{\mathbf{w}}(\xi)\mathbf{w}'(\xi))}{\sigma^2(\xi)}\,. \tag{3}$$

Since $\sigma(\xi)$ is a polynomial of degree $2m$, the cumulative arc length function

$$s(\xi) \;=\; \int_0^{\xi} \sigma(t)\;\mathrm{d}t$$

is likewise just a polynomial in ξ, of degree $2m+1$.

A planar PH quintic is obtained by choosing a quadratic polynomial $\mathbf{w}(\xi)$, with Bernstein coefficients $\mathbf{w}_0, \mathbf{w}_1, \mathbf{w}_2$. On integrating (2), the Bézier control points $\mathbf{p}_k = x_k + \mathrm{i}\,y_k$ of the resulting PH quintic

$$\mathbf{r}(\xi) \;=\; \sum_{k=0}^{5} \mathbf{p}_k \binom{5}{k} (1-\xi)^{5-k}\xi^k$$

may be expressed [7] as

$$\begin{aligned}
\mathbf{p}_1 &= \mathbf{p}_0 + \frac{1}{5}\,\mathbf{w}_0^2\,, \\
\mathbf{p}_2 &= \mathbf{p}_1 + \frac{1}{5}\,\mathbf{w}_0\mathbf{w}_1\,, \\
\mathbf{p}_3 &= \mathbf{p}_2 + \frac{1}{5}\,\frac{2\mathbf{w}_1^2 + \mathbf{w}_0\mathbf{w}_2}{3}\,, \\
\mathbf{p}_4 &= \mathbf{p}_3 + \frac{1}{5}\,\mathbf{w}_1\mathbf{w}_2\,, \\
\mathbf{p}_5 &= \mathbf{p}_4 + \frac{1}{5}\,\mathbf{w}_2^2\,,
\end{aligned} \tag{4}$$

where $\mathbf{p}_0$ is a free integration constant. The parametric speed polynomial

$$\sigma(\xi) \;=\; \sum_{k=0}^{4} \sigma_k \binom{4}{k} (1-\xi)^{4-k}\xi^k$$

has the Bernstein coefficients

$$\begin{aligned}
\sigma_0 &= |\mathbf{w}_0|^2\,, \quad \sigma_1 \;=\; \mathrm{Re}(\overline{\mathbf{w}}_0\mathbf{w}_1)\,, \\
\sigma_2 &= \frac{2|\mathbf{w}_1|^2 + \mathrm{Re}(\overline{\mathbf{w}}_0\mathbf{w}_2)}{3}\,, \\
\sigma_3 &= \mathrm{Re}(\overline{\mathbf{w}}_1\mathbf{w}_2)\,, \quad \sigma_4 \;=\; |\mathbf{w}_2|^2\,,
\end{aligned} \tag{5}$$

and the total arc length is

$$L \;=\; s(1) \;=\; \frac{\sigma_0 + \sigma_1 + \sigma_2 + \sigma_3 + \sigma_4}{5}\,. \tag{6}$$

3 The interpolation problem

Consider the construction of a planar PH quintic $\mathbf{r}(\xi)$, $\xi \in [\,0,1\,]$ with given end points $\mathbf{q}_0, \mathbf{q}_1$, end tangents $\mathbf{t}_0 = \exp(\mathrm{i}\,\theta_0)$, $\mathbf{t}_1 = \exp(\mathrm{i}\,\theta_1)$ where $\theta_0, \theta_1 \in (-\pi, +\pi\,]$, and arc length L. To facilitate the analysis, it is convenient to use "canonical form" data with $\mathbf{q}_0 = 0$, $\mathbf{q}_1 = 1$. Upon setting $\Delta\mathbf{q} = \mathbf{q}_1 - \mathbf{q}_0$ with $\ell = |\Delta\mathbf{q}|$ and $\alpha = \arg(\Delta\mathbf{q})$, a transformation of given data to canonical form is achieved by (1) subtracting $\mathbf{q}_0$ from $\mathbf{q}_0$, $\mathbf{q}_1$; (2) dividing $\mathbf{q}_1$ by $\ell\exp(\mathrm{i}\,\alpha)$; (3) multiplying $\mathbf{t}_0$, $\mathbf{t}_1$ by $\exp(-\mathrm{i}\,\alpha)$; and (4) dividing L by ℓ.

The canonical form reduction adopted here has been previously used [13] in the context of first–order Hermite interpolation by planar PH quintics. It amounts to adoption of new coordinates (specified by a translation, scaling, and rotation of the original coordinates), that eliminates the end points $\mathbf{q}_0, \mathbf{q}_1$ as input variables, leaving only the transformed tangent angles θ_0, θ_1 and arc length L as free parameters. It should be noted that other transformations — e.g., a mapping that makes $\mathbf{t}_0$ and $\mathbf{t}_1$ symmetric relative to the real axis, but maintains a general orientation for $\Delta\mathbf{q}$ — are possible, yielding formulations different from but essentially equivalent to those in Proposition 1 below.

Once the canonical form interpolation problem is solved, the solution can be mapped to the original coordinate system by multiplying the $\mathbf{w}_0, \mathbf{w}_1, \mathbf{w}_2$ coefficients, as computed below, by the factor $\sqrt{\ell}\,\exp(\mathrm{i}\,\frac{1}{2}\alpha)$ and taking $\mathbf{p}_0 = \mathbf{q}_0$ in (4). For brevity, we focus on the generic case with $\theta_1 \neq \pm\,\theta_0$ — the cases of parallel end tangents ($\theta_1 = \theta_0$) and symmetric tangents ($\theta_1 = -\,\theta_0$) are treated separately in Remarks 4 and 5 below.

Remark 1. For canonical–form data, there is obviously no solution if $L < 1$, and a trivial straight–line solution if $L = 1$ and $\theta_0 = \theta_1 = 0$ or $\theta_0 = \theta_1 = \pi$. It is assumed henceforth that $L > 1$ and θ_0, θ_1 are not both 0 or π.

From expressions (3), the end–point tangents of $\mathbf{r}(\xi)$ are

$$\mathbf{t}(0) \;=\; \frac{\mathbf{w}_0^2}{|\mathbf{w}_0|^2} \;=\; \exp(\mathrm{i}\,\theta_0)\,, \quad \mathbf{t}(1) \;=\; \frac{\mathbf{w}_2^2}{|\mathbf{w}_2|^2} \;=\; \exp(\mathrm{i}\,\theta_1)\,. \tag{7}$$

As previously stated, the condition $|\mathbf{r}'(0)| = |\mathbf{r}'(1)|$ is imposed here to ensure symmetric solutions for symmetric data. Hence, writing

$$\mathbf{w}_0 \;=\; w\exp(\mathrm{i}\tfrac{1}{2}\theta_0)\,, \quad \mathbf{w}_1 \;=\; u + \mathrm{i}\,v\,, \quad \mathbf{w}_2 \;=\; w\exp(\mathrm{i}\tfrac{1}{2}\theta_1)\,, \tag{8}$$

with $w \neq 0$, the tangent constraints (7) are satisfied. Now for canonical–form data, with $\mathbf{r}(0) = 0$ and $\mathbf{r}(1) = 1$, interpolation of the end points yields the condition

$$\int_0^1 \mathbf{r}'(\xi)\,\mathrm{d}\xi \;=\; \frac{1}{5}\left[\,\mathbf{w}_0^2 + \mathbf{w}_0\mathbf{w}_1 + \frac{2\mathbf{w}_1^2 + \mathbf{w}_0\mathbf{w}_2}{3} + \mathbf{w}_1\mathbf{w}_2 + \mathbf{w}_2^2\,\right] \;=\; 1\,,$$

or equivalently

$$2\mathbf{w}_1^2 + 3(\mathbf{w}_0 + \mathbf{w}_2)\mathbf{w}_1 + 3\mathbf{w}_0^2 + 3\mathbf{w}_2^2 + \mathbf{w}_0\mathbf{w}_2 \;=\; 15\,. \tag{9}$$

Also, from (5) and (6), requiring the interpolant to have a specified arc length L yields the condition

$$2|\mathbf{w}_1|^2 + 3\,\mathrm{Re}((\overline{\mathbf{w}}_0 + \overline{\mathbf{w}}_2)\mathbf{w}_1) + 3\,|\mathbf{w}_0|^2 + 3\,|\mathbf{w}_2|^2 + \mathrm{Re}(\overline{\mathbf{w}}_0\mathbf{w}_2) \;=\; 15L\,. \quad (10)$$

It is convenient to introduce the notations

$$(c_0, s_0) \;:=\; (\cos\tfrac{1}{2}\theta_0, \sin\tfrac{1}{2}\theta_0) \quad \text{and} \quad (c_1, s_1) \;:=\; (\cos\tfrac{1}{2}\theta_1, \sin\tfrac{1}{2}\theta_1)\,,$$

and to set $\theta_0 = \theta_m - \delta\theta$ and $\theta_1 = \theta_m + \delta\theta$, where

$$\theta_m \;:=\; \tfrac{1}{2}(\theta_0 + \theta_1) \qquad \text{and} \qquad \delta\theta \;:=\; \tfrac{1}{2}(\theta_1 - \theta_0)\,, \quad (11)$$

so that $\theta_m \in (-\pi, +\pi\,]$ and $\delta\theta \in (-\pi, +\pi)$ when $\theta_0, \theta_1 \in (-\pi, +\pi\,]$.

Proposition 1. *In canonical form, the interpolants to the prescribed data θ_0, θ_1 and L are specified by the coefficients* (8)*, where the values u, v, w are the real solutions to the system of quadratic equations*

$$\begin{aligned}
4u^2 + 6(c_0 + c_1)uw + (6c_0^2 + 6c_1^2 + 2c_0c_1)w^2 - 15(L+1) \;&=\; 0\,,\\
4uv + 3(s_0 + s_1)uw + 3(c_0 + c_1)vw + (6c_0s_0 + 6c_1s_1 + c_0s_1 + c_1s_0)w^2 \;&=\; 0\,,\\
4v^2 + 6(s_0 + s_1)vw + (6s_0^2 + 6s_1^2 + 2s_0s_1)w^2 - 15(L-1) \;&=\; 0\,.
\end{aligned}$$

Proof. Substituting (8) into (9) and (10), and taking the real and imaginary parts of the former, yields the system of real equations

$$\begin{aligned}
&2(u^2 - v^2) + 3(c_0u - s_0v)w + 3(c_1u - s_1v)w\\
&\qquad + 3(c_0^2 - s_0^2)w^2 + 3(c_1^2 - s_1^2)w^2 + (c_0c_1 - s_0s_1)w^2 \;=\; 15\,,\\
&4uv + 3(s_0u + c_0v)w + 3(s_1u + c_1v)w\\
&\qquad + 6c_0s_0w^2 + 6c_1s_1w^2 + (c_0s_1 + c_1s_0)w^2 \;=\; 0\,,\\
&2(u^2 + v^2) + 3(c_0u + s_0v)w + 3(c_1u + s_1v)w\\
&\qquad + 6w^2 + (c_0c_1 + s_0s_1)w^2 \;=\; 15L\,.
\end{aligned}$$

Upon replacing the first and third equations by their sum and difference, and invoking some basic trigonometric relations, these equations simplify to the form specified in Proposition 1. ∎

Remark 2. The equations in Proposition 1 define three quadric surfaces (of which two are cylindrical) with at most eight distinct real intersection points corresponding to their solutions (u, v, w). However, these solutions define at most four distinct planar PH quintics satisfying the data θ_0, θ_1 and L — since each real solution (u, v, w) has a counterpart $(-u, -v, -w)$ that defines the same curve. Thus, it suffices to consider only those solutions with $w > 0$.

The *homotopy method* [2, 3, 24, 25] is one possible approach to solving the equations in Proposition 1. If $f_1(u, v, w) = 0$, $g_1(u, v, w) = 0$, $h_1(u, v, w) = 0$ denote these equations, and $f_0(u, v, w) = 0$, $g_0(u, v, w) = 0$, $h_0(u, v, w) = 0$ is a set of simplified "initial" equations with known distinct roots, a homotopy parameter $\lambda \in [\,0, 1\,]$ is introduced, and the roots of the system

$$\begin{aligned} f_\lambda(u, v, w) &:= (1 - \lambda)\, f_0(u, v, w) + \lambda\, f_1(u, v, w) = 0\,, \\ g_\lambda(u, v, w) &:= (1 - \lambda)\, g_0(u, v, w) + \lambda\, g_1(u, v, w) = 0\,, \\ h_\lambda(u, v, w) &:= (1 - \lambda)\, h_0(u, v, w) + \lambda\, h_1(u, v, w) = 0\,, \end{aligned}$$

are tracked from their initial values ($\lambda = 0$) to the desired final values ($\lambda = 1$) using a numerical (e.g., predictor–corrector) method to increment λ.

However, the homotopy method is computationally expensive, and entails tracking all (real and complex) solutions. The following results demonstrate that the problem of determining just the real solutions can be reduced to the elementary task of solving a univariate quadratic equation.

Proposition 2. *Interpolants to the data θ_0, θ_1 and L are identified by values $w = \pm\sqrt{z}$, where z is a non–negative real root of the quadratic equation*

$$h(z) = a_2 z^2 + a_1 z + a_0 = 0\,, \tag{12}$$

with coefficients

$$\begin{aligned} a_2 &= 2(c_0 s_1 - c_1 s_0)^2\,, \\ a_1 &= 3\,[\,2(c_0 c_1 + s_0 s_1 - 3)L + 3(c_0^2 - s_0^2 + c_1^2 - s_1^2) - 2(c_0 c_1 - s_0 s_1)\,]\,, \\ a_0 &= 36(L^2 - 1)\,. \end{aligned} \tag{13}$$

Proof. The first and third equations in Proposition 1 can be solved to express u and v in terms of w as

$$u = \frac{-3(c_0 + c_1)w + \mu\sqrt{p(z)}}{4} \quad \text{and} \quad v = \frac{-3(s_0 + s_1)w + \nu\sqrt{q(z)}}{4} \tag{14}$$

where $\mu, \nu = \pm 1$ and we define

$$z \;:=\; w^2\,,$$

$$p(z) \;=\; 60(L+1) - (15c_0^2 + 15c_1^2 - 10c_0c_1)z\,, \tag{15}$$

$$q(z) \;=\; 60(L-1) - (15s_0^2 + 15s_1^2 - 10s_0s_1)z\,. \tag{16}$$

Substituting from (14) into the second equation and simplifying then gives

$$\mu\nu\,\sqrt{p(z)}\sqrt{q(z)} \;=\; 5(c_0s_1 + c_1s_0 - 3c_0s_0 - 3c_1s_1)z\,, \tag{17}$$

or

$$p(z)q(z) \;=\; 25(c_0s_1 + c_1s_0 - 3c_0s_0 - 3c_1s_1)^2z^2 \tag{18}$$

on squaring both sides to eliminate the indeterminate signs μ and ν. Finally, substituting for $p(z)$ and $q(z)$ and simplifying yields the quadratic equation (12) with the indicated coefficients. ■

For given values of $\theta_0, \theta_1 \in (-\pi, +\pi\,]$ and $L > 1$, it is clearly a trivial task to compute the roots z of equation (12). In fact, the following results serve to show that the two roots of (12) are always real and positive.

Lemma 1. *When $\theta_1 \neq \theta_0$, the coefficients* (13) *satisfy $a_2 > 0$, $a_1 < 0$, $a_0 > 0$.*

Proof : The condition $\theta_1 \neq \theta_0$, i.e., $\delta\theta \neq 0$, ensures that $a_2 > 0$. Likewise, $a_0 > 0$ from the assumption that $L > 1$. Finally, setting

$$f \;:=\; (c_0 - c_1)^2 + 2(c_0^2 + c_1^2)\,, \quad g \;:=\; (s_0 - s_1)^2 + 2(s_0^2 + s_1^2)\,, \tag{19}$$

we can re–write a_1 as

$$a_1 \;=\; -\,3\,[\,f(L-1) + g(L+1)\,]\,, \tag{20}$$

which is clearly non–positive. In fact a_1 is strictly negative, since $L > 1$ and $f = g = 0 \;\Rightarrow\; c_0 = s_0 = c_1 = s_1 = 0$, which is impossible. ■

Lemma 2. *When $\theta_1 \neq \theta_0$, the roots z of the quadratic equation* (12) *are real.*

Proof : Using the definitions (11) and the trigonometric identity

$$\cos\theta_0 + \cos\theta_1 \;=\; 2\cos\theta_m \cos\delta\theta\,,$$

the coefficients of (12) can be expressed as

$$\begin{aligned} a_2 &= 2\,\sin^2\delta\theta\,, \\ a_1 &= 6\,[\,(\cos\delta\theta - 3)L + (3\cos\delta\theta - 1)\cos\theta_m\,]\,, \\ a_0 &= 36\,(L^2-1)\,. \end{aligned} \tag{21}$$

Note that a_2 vanishes only if $\sin\delta\theta = 0$, which corresponds to the excluded case $\theta_1 = \theta_0$. By routine manipulations, the discriminant $\Delta = a_1^2 - 4a_0a_2$ of equation (12) can be re–formulated as the non–negative expression

$$\Delta \;=\; 36\,[\,(3\cos\delta\theta - 1)L + (\cos\delta\theta - 3)\cos\theta_m\,]^2 \;+\; 288\sin^2\delta\theta\,\sin^2\theta_m\,. \tag{22}$$

Thus, since Δ is evidently non–negative, the roots of (12) are real. ∎

Lemma 3. *When $\theta_1 \neq \theta_0$, the roots z of equation* (12) *are distinct except in the singular case identified by the conditions*[1]

$$\sin\theta_m \;=\; 0 \qquad \text{and} \qquad \cos\delta\theta \;=\; \frac{L\pm 3}{3L\pm 1}\,, \tag{23}$$

in which equation (12) *has the double root*

$$z \;=\; \frac{3}{2}\,(3L\pm 1)\,. \tag{24}$$

Proof : The roots of (12) are coincident when $\Delta = 0$. For this to occur, both terms on the right in (22) must vanish. Since $\sin\delta\theta \neq 0$ by assumption, we must have $\sin\theta_m = 0$ and hence $\cos\theta_m = \pm 1$. Substituting for $\cos\theta_m$ into the first term then gives the second condition in (23). Under these conditions, equation (12) reduces to

$$4(L^2-1)\left[\,\frac{2\,z}{3L\pm 1} - 3\,\right]^2 \;=\; 0\,,$$

and therefore has the value (24) as a double root. ∎

Note that the condition $\sin\theta_m = 0$ in (23) implies that the end–tangents are symmetrically disposed about the line segment $[\,0,1\,]$ — i.e., $\theta_1 = -\,\theta_0$ (this special case is dealt with in Remark 5 below). Also, when $\theta_m = 0$, the second condition in (23) defines a valid $\cos\delta\theta$ value for all $L > 1$.

[1] The same choice of sign must used in equations (23) and (24).

Remark 3. When $\theta_1 \neq \theta_0$, the roots

$$z_\pm \;=\; \frac{-\,a_1 \,\pm\, \sqrt{a_1^2 - 4a_2a_0}}{2a_2} \tag{25}$$

of equation (12) are both positive. Since $a_2, -a_1, a_0 > 0$ by Lemma 1, when $\Delta = a_1^2 - 4a_2a_0 \neq 0$ we have $\sqrt{\Delta} < -\,a_1$, so z_- and z_+ are both positive, with $z_- < z_+$. When $\Delta = 0$, on the other hand, $z_- = z_+ = -\,a_0/a_1 > 0$.

Lemma 4. *Among the solutions* (25) *of equation* (12)*, only the smaller root* z_- *yields real solutions to the system of equations in Proposition 1.*

Proof : Although equation (12) is satisfied by two distinct positive real values of $z = w^2$ (distinct when $\Delta \neq 0$), the expressions (15) and (16) must be non–negative to yield real u, v values from (14). These expressions can be written in terms of the quantities (19) as

$$p(z) \;=\; 60(L+1) - 5fz\,, \quad q(z) \;=\; 60(L-1) - 5gz\,,$$

and they define decreasing linear functions whose values change from positive to negative at the points

$$z_p \;=\; \frac{12(L+1)}{f} \qquad \text{and} \qquad z_q \;=\; \frac{12(L-1)}{g}\,, \tag{26}$$

respectively. Because $a_2, a_0 > 0$ and $a_1 < 0$, the graph of (12) is positive for $z < z_-$ and $z > z_+$ and negative for $z_- < z < z_+$, where the roots $z_\pm$ are specified by (25). Then if $h(z_p)$ and $h(z_q)$ are both non–positive, $p(z_-)$ and $q(z_-)$ are both non-negative, while $p(z_+)$ and $q(z_+)$ are both non-positive, as seen in Figure 1. With $a_2 = 2(c_0s_1 - c_1s_0)^2$, $a_1 = -\,3\,[\,f(L-1) + g(L+1)\,]$, $a_0 = 36(L^2-1)$, evaluating (12) at z_p and z_q and simplifying gives

$$h(z_p) \;=\; \frac{36(L+1)^2}{f^2}\,[\,8(c_0s_1 - c_1s_0)^2 - fg\,]\,,$$

$$h(z_q) \;=\; \frac{36(L-1)^2}{g^2}\,[\,8(c_0s_1 - c_1s_0)^2 - fg\,]\,,$$

so $h(z_p)$ and $h(z_q)$ are non–positive if $8(c_0s_1 - c_1s_0)^2 - fg \leq 0$. Substituting from (19) for f and g and simplifying, this condition can be reduced to

$$-\,[\,c_0s_1 + c_1s_0 - 3(c_0s_0 + c_1s_1)\,]^2 \;\leq\; 0\,,$$

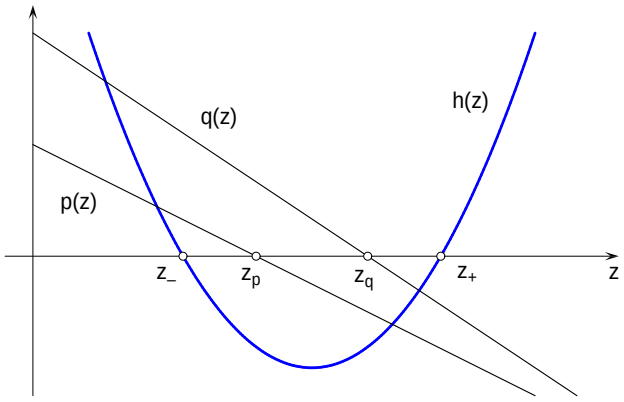

Figure 1: Schematic graphs of the quadratic function $h(z)$ with roots $z_\pm$ and the linear functions $p(z)$, $q(z)$ with roots z_p, z_q. The conditions $h(z_p) < 0$, $h(z_q) < 0$ are equivalent to $p(z_-) > 0$, $q(z_-) > 0$ and $p(z_+) < 0$, $q(z_+) < 0$.

which is obviously satisfied. Hence, only the solution z_- ensures non–negative values for $p(z)$ and $q(z)$. ■

Once the positive w values satisfying (12) are computed, appropriate signs μ and ν in (14) must be determined. Now the first and third of the equations in Proposition 1 are satisfied for any choice of μ and ν, but the second is only satisfied for those choices that are consistent with the condition (17). Thus, μ and ν must be of like or unlike sign, according to whether the expression on the right in (17) is positive or negative.

Proposition 3. *When $\theta_0 \neq \theta_1$, there are exactly two distinct interpolants to the canonical–form data θ_0, θ_1 and L.*

Proof : According to Lemma 4, among the two roots (25) of equation (12), only z_- identifies a real solution to the system of equations in Proposition 1. This yields the two values $w = \pm\sqrt{z_-}$, but from Remark 2 the negative value is superfluous. For the positive value there are, in general, two sign pairs μ, ν satisfying (17), and they define distinct interpolants. ■

In order to complete the analysis, we now address the two singular cases that arise when $\theta_1 = \theta_0$ and $\theta_1 = -\theta_0$.

Remark 4. In the case of parallel tangents with $\theta_1 = \theta_0$ ($= \theta$, say) we have $\theta_m = \theta$ and $\delta\theta = 0$, so $a_2 = 0$ and equation (12) then has the single real root

$$w \;=\; \sqrt{\frac{3(L^2-1)}{L-\cos\theta}}\,. \tag{27}$$

For this root, the choice of the signs μ, ν in (14) is again based on requiring their product to be of the same sign as the right–hand side of (17) — namely, the same sign as $-\sin\theta$ in this particular case.

Remark 5. In the case of symmetric tangents with $\theta_1 = -\theta_0$ ($= \theta$, say) we have $\theta_m = 0$ and $\delta\theta = \theta$. In this case, the coefficient $c_0 s_1 + c_1 s_0 - 3c_0 s_0 - 3c_1 s_1$ on the right–hand side of (17) vanishes, so $h(z) = p(z)q(z)$ and its roots are just the roots of $p(z)$ and $q(z)$, namely $z = 12(L+1)/f$ and $z = 12(L-1)/g$, where f and g are defined by (19). For each value $w = \sqrt{z}$, the corresponding u, v values are again determined by (14) provided that $q(z)$ is non–negative if $p(z) = 0$, and vice–versa (only one sign choice arises each case).

Several authors [22, 27] have considered the approximation order of PH curve interpolants to discrete data, based on rather complicated asymptotic analyses. Such an analysis may be possible in the present context, although the presence of an integral constraint is an additional complication. However, we emphasize that the method described herein is intended as a curve *design* scheme, rather than as a means to approximate other given curves. The exact computational advantages of PH curves are of doubtful value if, in fact, they arose from the approximation of other prescribed curves.

4 Algorithm and computed examples

The following algorithm outline summarizes the procedure for constructing planar PH quintic interpolants to given end points $\mathbf{q}_0, \mathbf{q}_1$ and unit tangents $\mathbf{t}_0, \mathbf{t}_1$ with specified arc lengths L. For brevity, the algorithm considers only the generic case $\theta_1 \neq \pm\theta_0$ (branching conditions can easily be incorporated to accommodate these special cases, as described in Remarks 4 and 5).

Algorithm

input: initial/final points $\mathbf{q}_0, \mathbf{q}_1$, tangents $\mathbf{t}_0, \mathbf{t}_1$, and arc length L.

1. convert the input data to canonical form by setting $\ell = |\mathbf{q}_1 - \mathbf{q}_0|$ and $\alpha = \arg(\mathbf{q}_1 - \mathbf{q}_0)$, and (a) subtracting $\mathbf{q}_0$ from $\mathbf{q}_0$, $\mathbf{q}_1$; (b) dividing $\mathbf{q}_1$ by $\ell \exp(\mathrm{i}\,\alpha)$; (c) dividing $\mathbf{t}_0$, $\mathbf{t}_1$ by $\exp(\mathrm{i}\,\alpha)$; and (d) dividing L by ℓ;

2. set $\theta_m = \frac{1}{2}(\theta_0+\theta_1), \delta\theta = \frac{1}{2}(\theta_1-\theta_0)$, $c_i = \cos\frac{1}{2}\theta_i, s_i = \sin\frac{1}{2}\theta_i$ for $i = 0, 1$;

3. (a) compute the coefficients (21) of the quadratic equation (12) and its root z_- specified by (25), and set $w = \sqrt{z_-}$;

4. identify whether like or unlike signs μ and ν yield satisfaction of (17);

5. for each combination μ, ν, w thus identified, compute the corresponding u and v values from expressions (14);

6. for each combination of u, v, w values thus obtained, form the complex coefficients $\mathbf{w}_0, \mathbf{w}_1, \mathbf{w}_2$ from expressions (8);

7. map each canonical–form solution to the original coordinate system by multiplying each of the coefficients (8) with $\sqrt{\ell}\,\exp(\mathrm{i}\,\frac{1}{2}\alpha)$, and compute the control points (4) with $\mathbf{p}_0 = \mathbf{q}_0$.

output: two planar quintic PH curves $\mathbf{r}(\xi)$ that satisfy $\mathbf{r}(0) = \mathbf{q}_0$, $\mathbf{r}(1) = \mathbf{q}_1$, $\mathbf{r}'(0) = w^2\mathbf{t}_0$, $\mathbf{r}'(1) = w^2\mathbf{t}_1$, with the prescribed arc length L.

The following examples[2] serve to illustrate the above algorithm in operation, and also the special instances covered by Remarks 4 and 5. The first example illustrates that, for "reasonable" L values, one of the two solutions yields a smooth curve while the other exhibits an undesirable looping behavior (but is still a correct formal solution to the interpolation problem). This behavior is typical [1, 13] of the multiple solutions to PH curve interpolation problems. The "good" solution may be identified as the one with the least value for the *absolute rotation index* defined by

$$R_{\mathrm{abs}} \;=\; \int_0^1 |\kappa(\xi)|\,\sigma(\xi)\,\mathrm{d}\xi\,, \tag{28}$$

which admits closed–form evaluation, as described in [5, 13].

[2]For simplicity, canonical–form input data will be assumed in the examples, so step 1 of the algorithm is bypassed.

Example 1. The two formal interpolants to the data $\theta_0 = 60°$, $\theta_1 = -135°$, and $L = 1.5$ are shown in Figure 2. The "good" solution — with the smaller value of (28) — has a very pleasing shape, while the looping solution must be rejected. To six decimal places, the good solution corresponds to the values

$$u = 1.803045\,, \quad v = 0.249124\,, \quad w = 1.185161\,,$$

which define through (8) the complex coefficients

$$\begin{aligned} \mathbf{w}_0 &= 1.026379 + 0.592580\,\mathrm{i}\,, \\ \mathbf{w}_1 &= 1.803045 + 0.249124\,\mathrm{i}\,, \\ \mathbf{w}_2 &= 0.453541 - 1.094946\,\mathrm{i}\,, \end{aligned}$$

and the resulting control points are

$$\begin{aligned} \mathbf{p}_0 &= (0.000000, 0.000000)\,, \\ \mathbf{p}_1 &= (0.140461, 0.243285)\,, \\ \mathbf{p}_2 &= (0.481057, 0.508114)\,, \\ \mathbf{p}_3 &= (0.980535, 0.570891)\,, \\ \mathbf{p}_4 &= (1.198641, 0.198641)\,, \\ \mathbf{p}_5 &= (1.00000, 0.0000000)\,. \end{aligned}$$

The accuracy of the solution is illustrated by noting that, for the computed u, v, w values, the residuals for the equations in Proposition 1 are

$$-0.000000000000007\,, \quad -0.000000000000001\,, \quad -0.000000000000001\,,$$

and the arc length of the interpolant, computed from (5) and (6), is

$$L = 1.500000000000000\,,$$

in agreement with the prescribed value to 15 decimal places.

The next example illustrates the behavior of interpolants with fixed θ_0, θ_1 and increasing L values. Although formal solutions exist for any L greater than 1, it is clear that interpolants of reasonable shape cannot be expected if L is much greater than 1 (even the "good" solution may exhibit loops).

Example 2. For the convex data $\theta_0 = 45°$ and $\theta_1 = -60°$ and the inflectional data $\theta_0 = -30°$ and $\theta_1 = -60°$ Figure 3 illustrates the interpolants for the sequence of increasing L values $1.1, 1.2, \ldots, 1.6$.

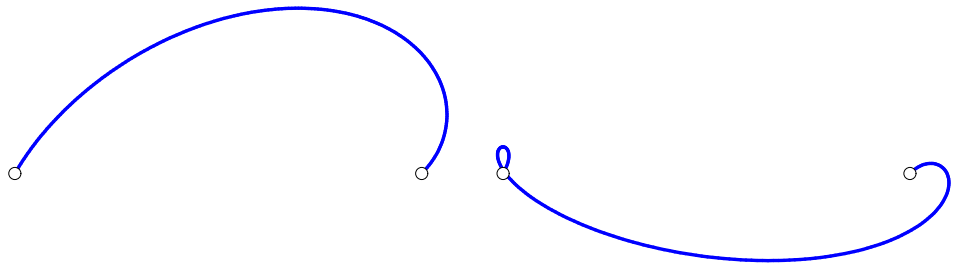

Figure 2: The two solutions for the data in Example 1. The looping solution is rejected on the basis of a much higher value for the shape measure (28).

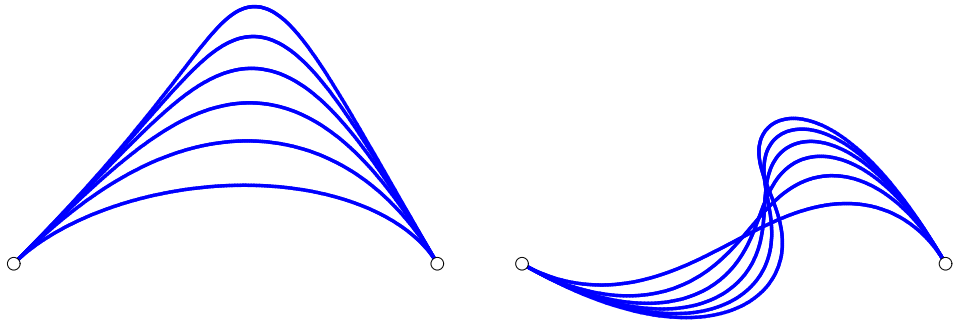

Figure 3: Interpolants for the Example 2 convex and inflectional data, with increasing arc lengths $L = 1.1, \ldots, 1.6$ (only the good solutions are shown).

Example 3. As an example of the parallel–tangents case, consider the data $\theta_1 = \theta_0 = 45^\circ$ and $L = 1.5$, for which the two formal solutions are shown in Figure 4. In this case, equation (27) gives the unique w value

$$w \;=\; \sqrt{\frac{15}{6 - 2\sqrt{2}}}\,,$$

and (15) and (16) become $p(z) = 10(15 - z)$ and $q(z) = 10(3 - z)$, which are both positive for $z = w^2$. Finally, since the right–hand side of (17) becomes $-\sqrt{2}\,z$, opposite signs must be chosen for μ and ν.

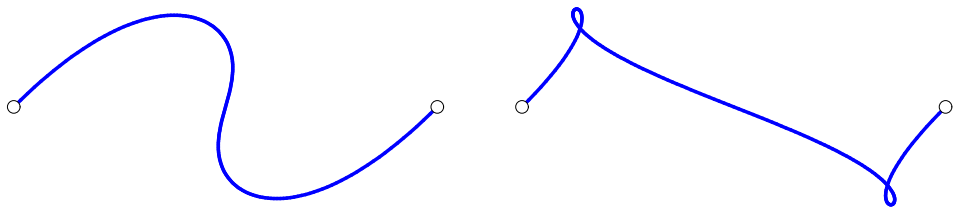

Figure 4: The formal solutions for the case of parallel tangents (see Remark 4) in Example 3 with $\theta_1 = \theta_0 = 45^\circ$, $L = 1.5$. The looping solution is discarded.

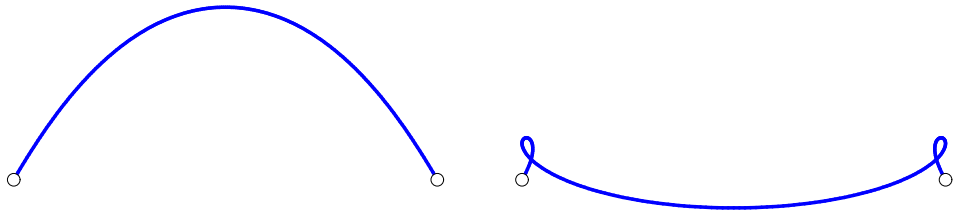

Figure 5: The formal solutions for the case of symmetric tangents (Remark 5) in Example 4 ($\theta_0 = -\,\theta_1 = 60^\circ$, $L = 1.35$). The looping solution is discarded.

Example 4. As an example of the symmetric–tangents case, consider the data $\theta_0 = -\,\theta_1 = 60^\circ$ and $L = 1.35$, for which the two solutions are shown in Figure 5. In this case, the functions (15) and (16) become $p(z) = 141 - 15\,z$ and $q(z) = 21 - 10\,z$, and their roots (26) are

$$z_p \;=\; 9.4 \quad \text{and} \quad z_q \;=\; 2.1\,.$$

Since $p(z_q)$ is positive and $q(z_p)$ is negative, we take $w = \sqrt{z_q}$ and exercise the two choices for the sign μ in (14) to obtain the interpolants in Figure 5.

Figure 6 compares the good PH quintic interpolants in Examples 1 and 3 with the unique "ordinary" cubics having the same end points and derivatives (note that it is not possible to impose the arc length constraint on the cubics). As usual with such comparisons, the PH quintics exhibit better overall shape, with milder curvature variations, for prescribed end data [8].

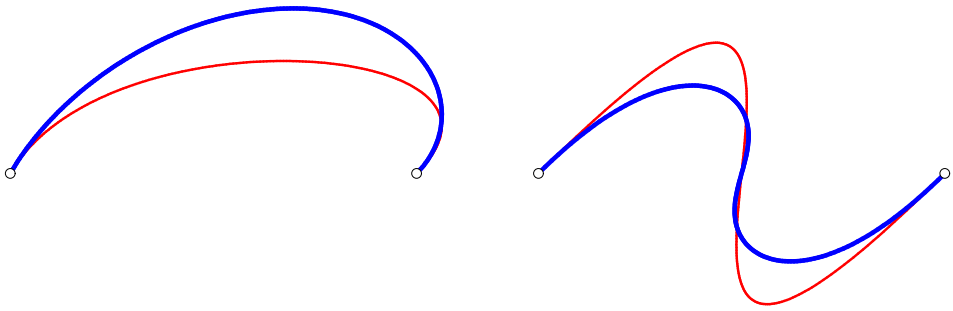

Figure 6: Comparison of the good interpolants in Examples 1 and 3 (blue) with the "ordinary" cubics (red) having the same end points and derivatives.

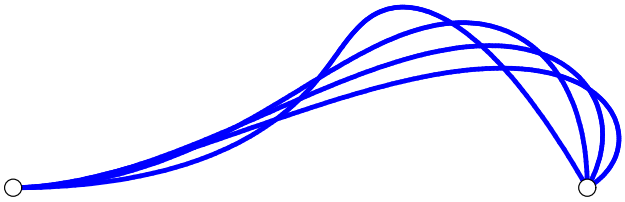

Figure 7: The good interpolants corresponding to the fixed values $\theta_0 = 0°$, $L = 1.25$ and successive θ_1 values $-60°, -90°, -120°, -150°$ in Example 5.

Example 5. Consider the data $\theta_0 = 0°$ and $L = 1.25$ with the successive values $-60°, -90°, -120°, -150°$ of θ_1, for which the good interpolants are plotted in Figure 7. As $\theta_1 \to 0°$ in this case (i.e., both end tangents approach parallelism with the end–point displacment), even the good interpolant is no longer satisfactory, since the relatively large value of L is incompatible with parallelism of the end tangents and the displacement vector.

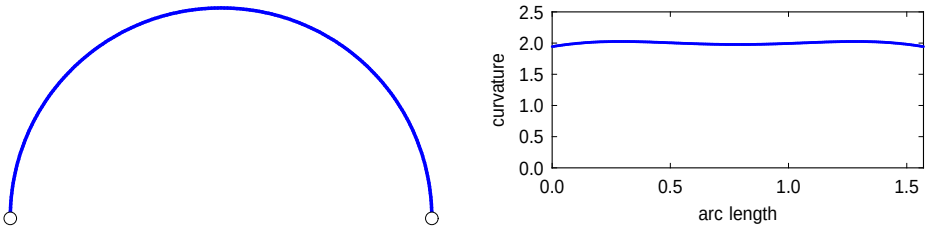

Figure 8: Left: the good solution for data $\theta_0 = -\theta_1 = 90°$, $L = \frac{1}{2}\pi$ from a unit semi–circle — to the scale of the plot, the interpolant is indistinguishable from the exact semi–circle. Right: curvature variation along the interpolant.

Example 6. Finally, consider the data $\theta_0 = -\theta_1 = 90°$ and $L = \frac{1}{2}\pi$ from a semi–circle of unit diameter. Figure 8 shows the good solution in this case, which is indistinguishable from the exact semi–circle on the scale of the plot. To six decimal places, this solution is determined by the values

$$u \;=\; 1.539536\,, \quad v \;=\; 0.000000\,, \quad w \;=\; 1.308583\,,$$

with corresponding complex coefficients

$$\begin{aligned} \mathbf{w}_0 &= 0.925308 + 0.925308\,\mathrm{i}\,, \\ \mathbf{w}_1 &= 1.539536 + 0.000000\,\mathrm{i}\,, \\ \mathbf{w}_2 &= 0.925308 - 0.925308\,\mathrm{i}\,, \end{aligned}$$

and control points

$$\begin{aligned} \mathbf{p}_0 &= (0.000000, 0.000000)\,, \\ \mathbf{p}_1 &= (0.000000, 0.342478)\,, \\ \mathbf{p}_2 &= (0.284909, 0.627387)\,, \\ \mathbf{p}_3 &= (0.715091, 0.627387)\,, \\ \mathbf{p}_4 &= (1.000000, 0.342478)\,, \\ \mathbf{p}_5 &= (1.00000, 0.0000000)\,. \end{aligned}$$

A quantitative analysis of the interpolant shows that the distance of its points from the center $(0.5, 0.0)$ lie in the range $[\,0.499141, 0.500545\,]$, corresponding to a deviation of $< 0.2\%$ from the exact circle radius $r = 0.5$. Figure 8 also shows the curvature plot for the interpolant — the maximum deviation from the value $\kappa = 2$ for the exact circle is $< 3\%$, and occurs at the end–points.

5 Closure

In free–form curve design, an exact imposition of a prescribed arc length may be desired to ensure satisfaction of certain geometrical or physical constraints. Since it is impossible (except in trivial instances) to exactly compute the arc lengths of general polynomial/rational parametric curves, such a requirement can only be approximately satisfied, through overtly numerical methods.

Taking advantage of the distinctive properties of Pythagorean–hodograph (PH) curves, an elementary and exact solution to the problem of constructing a planar curve with given end points and tangents, and a specified arc length, has been developed herein. Exploiting the complex PH curve representation, and a reduction of the given data to canonical form, yields a very simple and efficient algorithm, that requires only elementary algebraic and trigonometric computations and the solution of a single quadratic equation. Furthermore, the computed solutions are found to satisfy the end conditions and arc length constraint to an accuracy approaching machine precision. By construction, the interpolants inherit all the advantageous features of PH curves, including rational tangents and normals, curvatures, and offset curves, and real–time interpolator algorithms for precision motion control applications.

The present study is only a preliminary investigation into the possibility of interpolating both local and global geometrical properties, by appealing to the advantageous features of PH curves. It has the virtue of accommodating an exact and efficient closed–form solution that admits a very straightforward implementation. There are several interesting directions in which the present results may possibly be extended, including: (i) interpolation of higher–order local data, such as curvature; (ii) the extension from planar to spatial data; and (iii) the imposition of values for (or minimization of) higher–order global shape measures, such as the bending energy. However, these are analytically and computationally more challenging problems, which are unlikely to admit solutions as simple and exact as obtained in the present context.

References

[1] G. Albrecht and R. T. Farouki (1996), Construction of C^2 Pythagorean–hodograph interpolating splines by the homotopy method, *Adv. Comp. Math.* **5**, 417–442.

[2] E. L. Allgower and K. Georg (1990), *Numerical Continuation Methods: An Introduction*, Springer, Berlin.

[3] E. L. Allgower and K. Georg (1993), Continuation and path following, *Acta Numerica* **2**, 1–64.

[4] C. de Boor, K. Höllig, and M. Sabin (1987), High accuracy geometric Hermite interpolation, *Comput. Aided Geom. Design* **4**, 269–278.

[5] B. Dong and R. T. Farouki, Algorithm 952: `PHquintic`: A library of basic functions for the construction and analysis of planar quintic Pythagorean–hodograph curves, *ACM Trans. Math. Software* **41** (4), Article 28 (2015)

[6] G. Farin (2008), Geometric Hermite interpolation with circular precision, *Comput. Aided Design* **40**, 476–479.

[7] R. T. Farouki (1994), The conformal map $z \rightarrow z^2$ of the hodograph plane, *Comput. Aided Geom. Design* **11**, 363–390.

[8] R. T. Farouki (2008), *Pythagorean–Hodograph Curves: Algebra and Geometry Inseparable*, Springer, Berlin.

[9] R. T. Farouki, M. al–Kandari, and T. Sakkalis (2002), Hermite interpolation by rotation–invariant spatial Pythagorean–hodograph curves, *Adv. Comp. Math.* **17**, 369–383.

[10] R. T. Farouki, C. Giannelli, C. Manni, and A. Sestini (2008), Identification of spatial PH quintic Hermite interpolants with near–optimal shape measures, *Comput. Aided Geom. Design* **25**, 274–297.

[11] R. T. Farouki, J. Manjunathaiah, D. Nicholas, G–F. Yuan, and S. Jee (2008), Variable–feedrate CNC interpolators for constant material removal rates along Pythagorean–hodograph curves, *Comput. Aided Design* **30**, 631–640.

[12] R. T. Farouki, J. Manjunathaiah, and G–F. Yuan (1999), G codes for the specification of Pythagorean–hodograph tool paths and associated feedrate functions on open–architecture CNC machines, *Int. J. Machine Tools Manufac.* **39**, 123–142.

[13] R. T. Farouki and C. A. Neff (1995), Hermite interpolation by Pythagorean–hodograph quintics, *Math. Comp.* **64**, 1589–1609.

[14] R. T. Farouki and T. Sakkalis (1990), Pythagorean hodographs, *IBM J. Res. Develop.* **34**, 736–752.

[15] R. T. Farouki and S. Shah, Real–time CNC interpolators for Pythagorean–hodograph curves (1996), *Comput. Aided Geom. Design* **13**, 583–600.

[16] Z. Habib and M. Sakai (2007), G^2 Pythagorean hodograph quintic transition between two circles with shape control, *Comput. Aided Geom. Design* **24**, 252–266.

[17] C. Y. Han (2010), Geometric Hermite interpolation by monotone helical quintics, *Comput. Aided Geom. Design* **27**, 713–719.

[18] K. Höllig and J. Koch (1995), Geometric Hermite interpolation, *Comput. Aided Geom. Design* **12**, 567–580.

[19] K. Höllig and J. Koch (1996), Geometric Hermite interpolation with maximal order and smoothness, *Comput. Aided Geom. Design* **13**, 681–695.

[20] M. Huard, R. T. Farouki, N. Sprynski, and L. Biard (2014), C^2 interpolation of spatial data subject to arc–length constraints using Pythagorean–hodograph quintic splines, *Graph. Models* **76**, 30–42.

[21] G. Jaklič, J. Kozak, M. Krajnc, V. Vitrih, and E. Žagar (2012), An approach to geometric interpolation by Pythagorean–hodograph curves, *Adv. Comp. Math.* **37**, 123–150.

[22] G. Jaklič, J. Kozak, M. Krajnc, V. Vitrih, and E. Žagar (2014), Interpolation by G^2 quintic Pythagorean–hodograph curves, *Numer. Math. Theor. Meth. Appl.* **7**, 374–398.

[23] L. Lu (2015), Planar quintic G^2 Hermite interpolation with minimum strain energy, *J. Comput. Appl. Math.* **274**, 109–117.

[24] A. P. Morgan (1987), *Solving Polynomial Systems Using Continuation for Engineering and Scientific Problems*, Prentice–Hall, Englewood Cliffs, NJ.

[25] A. P. Morgan and A. Sommese (1987), Computing all solutions to polynomial systems using homotopy continuation, *Appl. Math. Comp.* **24**, 115–138.

[26] F. Pelosi, R. T. Farouki, C. Manni, and A. Sestini (2005), Geometric Hermite interpolation by spatial Pythagorean–hodograph cubics, *Adv. Comp. Math.* **22**, 325–352.

[27] Z. Šír, R. Feichtinger, and B. Jüttler (2006), Approximating curves and their offsets using biarcs and Pythagorean hodograph quintics, *Comput. Aided Design* **38**, 608–618.

[28] D. J. Walton and D. S. Meek (1998), G^2 curves composed of planar cubic and Pythagorean–hodograph spirals, *Comput. Aided Geom. Design* **15**, 547–566.

[29] D. J. Walton and D. S. Meek (2002), Planar G^2 transition with a fair Pythagorean hodograph quintic curve, *J. Comput. Appl. Math.* **138**, 109–126.

[30] L. Xu and J. Shi (2001), Geometric Hermite interpolation for space curves, *Comput. Aided Geom. Design* **18**, 817–829.

[31] X. Yang (2014), Geometric Hermite interpolation by logarithmic arc splines, *Comput. Aided Geom. Design* **31**, 701–711.

[32] J–H. Yong and F. Cheng (2004), Geometric Hermite curves with minimum strain energy, *Comput. Aided Geom. Design* **21**, 281–301.